AIAA JOURNAL
Vol. 40, No. 8, August 2002

Collapse of Rectangular Aluminum Plates with Axial Cracks

Edmundo Corona*
University of Notre Dame, Notre Dame, Indiana 46556
W. Allen Waters Jr.†
Lockheed Martin Space Operations, Hampton, Virginia 23681
and
James H. Starnes Jr.‡
NASA Langley Research Center, Hampton, Virginia 23681

Results of an experimental and numerical study of the residual strength of compression-loaded rectangular aluminum plates with longitudinal cracks are presented. The paper concentrates first on the experimental results and the numerical simulations of the experiments. The results of a parametric study to determine the effects of varying selected parameters on plate response are also presented. The results indicate that the response of the plates is characterized by a limit load instability that induces collapse. Experimental results show that the collapse loads of the plates depend on the location of the crack and that these loads are lower when the crack is located near a longitudinal edge. The numerical results agree with the experimental results. The results of the parametric study indicate that the dependence of the collapse load on crack length is most significant when the cracks are near a longitudinal edge. The collapse load of plates that are simply supported or clamped on all four edges show the same trends as the crack length increases, although the values are, as expected, different. Plates with edges constrained to remain straight in their planes had higher collapse loads than those with edges free to deform in plane. The degree of geometric imperfection sensitivity of the collapse load is not significantly affected by the presence of cracks for the cases considered.

Introduction

THE designs of some major structural components in transport aircraft are based on the fail-safe design philosophy. Fail-safe or damage-tolerant design implies that a structure containing some degree of damage can be operated safely. The achievement of safety goals requires damage tolerant design to include assessments of the maximum amount of damage that a structure can safely sustain (damage limit) and the rate of damage propagation. An inspection program must be developed to ensure that the extent of damage does not reach an unsafe level for limit load conditions.[1] Issues concerning the residual strength of rectangular flat plates with longitudinal cracks and their relationship to the estimation of the damage limit of structures are presented in the present paper.

Airframes are complex structures that include many structural components such as skin panels, bulkheads, stiffeners, frames, tear straps, etc. Accurate calculations of the effect of damage for entire fuselage or wing structures require complex models with sufficient structural detail, which include geometric and material nonlinearities. To investigate specific issues related to small-scale damage conditions such as skin cracks more easily, it is often convenient to consider the response of subassemblies such as fuselage sections or stiffened panels.[2,3] Further studies at an even more basic level have included the study of cracked cylindrical shells subjected to internal pressure and axial loads.[4]

The present paper investigates the response and collapse of elastic-plastic rectangular aluminum plates with longitudinal cracks subjected to uniaxial compressive loads and relates this response to the residual strength of the plates. The objective of this study is to determine the response of the plates and to investigate the effect of crack length and position on the collapse loads of the plates. The influence of aspect ratio, boundary conditions, and initial geometric imperfections are also addressed. The approach involves a limited experimental study and comparisons between experimental results and numerical predictions. A numerical parametric study is presented, where the effects of various factors that affect the response and collapse of the plates are assessed.

Received 1 June 2001; revision received 4 February 2002; accepted for publication 5 February 2002.

*Associate Professor, Department of Aerospace and Mechanical Engineering. Member AIAA.
†Aeronautical Engineer.
‡Senior Engineer for Structures and Materials. Fellow AIAA.

Test Specimens and Analysis Code

The geometry, loading, and boundary conditions of a typical test plate specimen are shown in Fig. 1. The plate has length L, width b, and thickness t. It contains a crack of length $2a$ aligned parallel to the long sides. The center of the crack is located half way along the length of the plate, but can be offset a distance e from the axial centerline as shown in Fig. 1. The plate is loaded in uniaxial compression. The boundary conditions are varied in the numerical study and are specified subsequently as necessary. In all calculations, however, the in-plane displacements of the edges of length b are constrained so that the edges remain straight and horizontal. The axial displacement v at the lower edge is equal to zero, and a uniform uniaxial end shortening δ is applied to the top edge.

The plate material is 2024-T3 bare aluminum alloy. Representing the elastic-plastic response of the material is essential because this problem involves collapse. The material stress-strain curve was obtained from material coupons cut from nominally 2.29-mm (0.090-in.)-thick plate along the rolling direction and is shown in Fig. 2.

The numerical results were generated using the finite element code STAGS (Structural Analysis of General Shells).[5] The formulation of the STAGS 410 element used in this study contains the necessary kinematic nonlinearities to study buckling and the nonlinear response of shells.[6] The elastic-plastic response of the material is calculated using the White–Besseling or mechanical sublayer model.[7,8] The uniaxial stress-strain curve of the material was discretized by straight segments (see Fig. 2).

Plate Response

Examples of the numerically calculated response of plates with cracks are presented to facilitate discussion of the experimental and numerical results generated in this study.

The net axial load P as a function of the axial shortening δ response of three plates with $L/b = 4$ and $b/t = 66.7$ is shown in

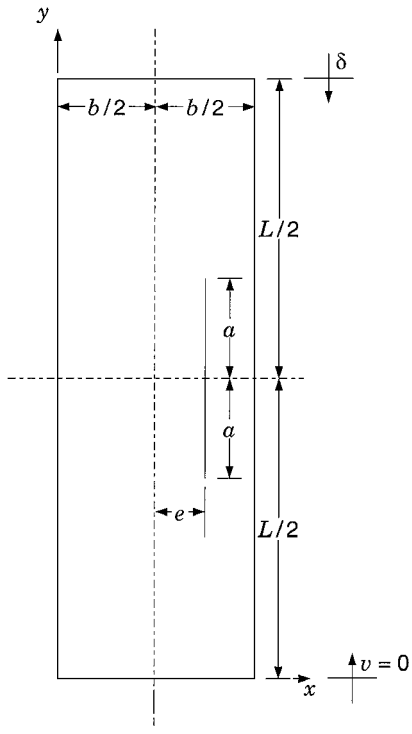

Fig. 1 Plate geometry and loading conditions.

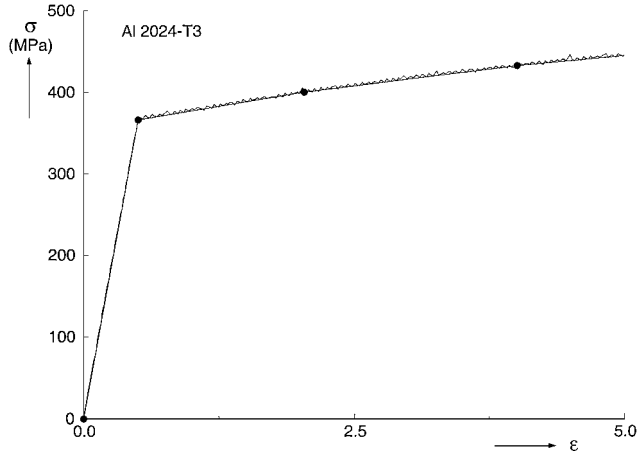

Fig. 2 Uniaxial stress-strain curve and fit.

Fig. 3. The plates are clamped on all edges, which prevents out-of-plane displacements. The in-plane boundary conditions allow the plate to expand in plane so that the total transverse load is equal to zero, and the sides of length L remain straight and vertical. The actual dimensions of the plates in the model are $L = 610$ mm (24 in.), $b = 152$ mm (6 in.), and $t = 2.29$ mm (0.090 in.). The load is normalized by the yield load of the plates. [$P_o = \sigma_o bt$, where $\sigma_o = 372$ MPa (54 ksi) is the 0.2% offset yield stress of the material.] The axial shortening is normalized by L. The numerical calculations are performed using a two-step process: 1) the first four bifurcation buckling loads and modes of the plate are calculated, and 2) the nonlinear response of the plate is calculated. In this step a linear combination of the four buckling modes is introduced as an initial geometric imperfection. The amplitude of each mode is 0.0375% of the width; therefore, $w_o/b = 0.15\%$ if all four modes had their maximum deflection at the same location. Nonetheless, w_o/b provides a reasonable approximation of the imperfection amplitude. The nonlinear analysis of the plate under compression is then performed until a maximum axial load is identified. The presence of the initial geometric imperfections ensures that the calculated response follows the stable postbuckling branch once the bifurcation load is exceeded. The optimum size of the finite elements used was determined to be 12.7×12.7 mm^2 (0.5×0.5 in.^{2}) from a mesh-convergence study. For example, using elements of size 6.4×6.4 mm^2 (0.25×0.25 in.^{2}) results in a reduction of the calculated maximum load on the order of 0.5%.

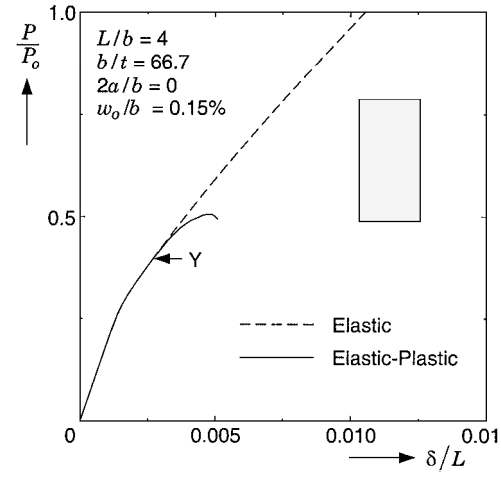

a) Plate with no crack

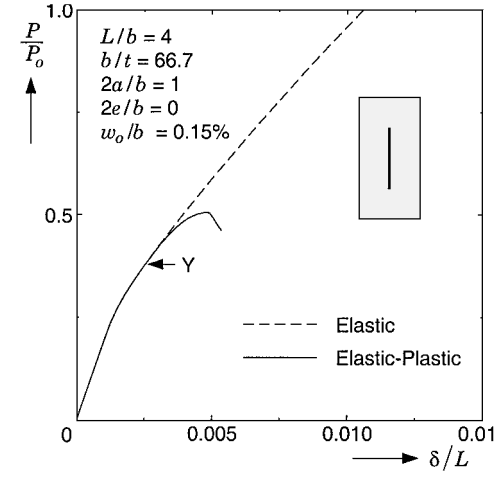

b) Plate with a crack at the center

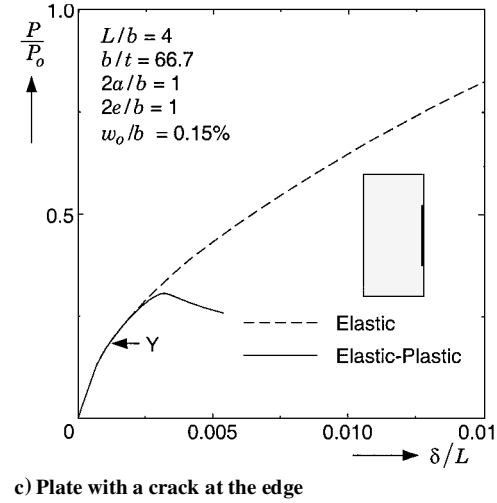

c) Plate with a crack at the edge

Fig. 3 Load-displacement response of three clamped plates.

The response of a plate with no crack is shown in Fig. 3a. The linearly elastic plate response is represented by the dashed line while the elastic-plastic plate response is the solid line. The two cases are identical until the load, in conjunction with the lateral deflections of the plate, induces yielding of the material at the point on the curve indicated by ***Y***. The bifurcation load of the plate occurs in the elastic range at $P/P_o = 0.281$. The "knee" of the curve at $P/P_o \approx 0.28$ therefore represents the decrease in stiffness of the plate caused by

the growth of lateral deflections. It is well known[9] that the postbuckling response of linearly elastic plates has a load-displacement response with a positive slope. Mode "jumping" instabilities[10] are possible in plates but do not occur in the load range up to $P/P_o = 1$ in this case. The elastic-plastic response, however, softens after yielding occurs and is characterized by a maximum in the load-displacement response at $P/P_o = 0.51$. This limit load instability defines the collapse load of such plates.

The response of a similar plate containing a crack with $2a/b = 1$ centered in the plate ($2e/b = 0$) is shown in Fig. 3b. Although normalizing the crack length by L might seem more natural, the parametric study results showed better correlation of the collapse loads for different values of L/b when $2a$ was normalized by b. The elastic and elastic-plastic responses are very similar to those in the preceding case. The bifurcation load occurs at $P/P_o = 0.239$, which is somewhat lower than for the plate without a crack, but the limit load $P/P_o = 0.495$ is nearly the same. The presence of the crack does not significantly affect the collapse load of the plate in this case.

The response of a similar plate to that shown in Fig. 3b is shown in Fig. 3c, with the crack located at the edge of the plate ($2e/b = 1$). In this case the bifurcation load occurs at a much lower value, $P/P_o = 0.127$, and the postbuckling response has less stiffness. This crack configuration results in yielding and collapse occurring at a much lower load than for the preceding two cases. The collapse load of this plate is $P/P_o = 0.302$, which is 40% lower than that of the plate with no crack. These results indicate that cracks located near the longitudinal edges of the plates can make the structural response more collapse critical.

Comparison of Experimental and Numerical Results

The experiments consisted of loading three plates to collapse. The specimens were machined from a sheet of 2024-T3 bare aluminum alloy with a thickness of 2.2 mm (0.088 in.). The specimens had a length $L = 527$ mm (20.75 in.) and a width $b = 152$ mm (6 in.). The dimension L of the specimens coincided with the rolling direction of the parent sheet. Two specimens contained saw-cut "cracks" of length $1.73b$ $(L/2)$. One specimen had no crack. The cracks had blunt tips, which delay possible crack extension. Indeed, no crack extension occurred in the plates tested. Numerical studies[11] considering the possibility of crack growth indicated that crack growth for the loading conditions considered is unlikely, even with sharp crack tips. The specimen used to measure the stress-strain curve in Fig. 2 was machined from the same parent sheet.

The specimens were installed in the load introduction fixture shown schematically in Fig. 4, which appropriately enforces the required boundary conditions.[12] The plate edges of length b were fitted into 9.5 mm ($\frac{3}{8}$ in.) deep slots at both ends of the fixture, which approximates clamped boundary conditions as shown in view B-B. The knife-edge side supports approximate simple support boundary conditions 6.4 mm ($\frac{1}{4}$ in.) inboard of the long edges, as shown in view A-A. The length of the side supports is 25.4 mm (1 in.) shorter than the plate specimen. The length of the side supports in combination with the 9.5 mm ($\frac{3}{8}$ in.) slots at the ends of the fixture allowed for a specimen end shortening of up to 6.4 mm ($\frac{1}{4}$ in.). The fixture and specimen were then placed between the platens of a 1300-kN (300-kip) uniaxial hydraulic testing machine. The fixture was carefully aligned in the testing machine to ensure as uniform a loading condition as possible. A shadow moiré interferometry system was used to monitor qualitatively the global pattern of out-of-plane displacements. Quantitative measurements of the out-of-plane displacements at discrete points were provided by an array of linearly variable differential transformers positioned behind the plate. A computer-based data-acquisition system recorded the axial load, the test machine cross-head displacement, and the output from all instrumentation. The uncertainty estimates in the reported load and displacement values are 1 and 0.5%, respectively.

The experiments were simulated using STAGS. The finite element models included all out-of-plane displacement and rotational constraints imposed by the fixture. A small geometric imperfection made up of the first four buckling modes and with an amplitude of $w_o/b = 0.15$ was introduced in the analysis. The possibility of crack extension was not considered in the numerical analysis.

The first experiment was conducted with a specimen without a crack. The out-of-plane displacement pattern indicated by the moiré method at the highest load recorded is shown in Fig. 5a. The calculated out-of-plane displacement contours at the limit load shown in Fig. 5b compare very well qualitatively with the experimental

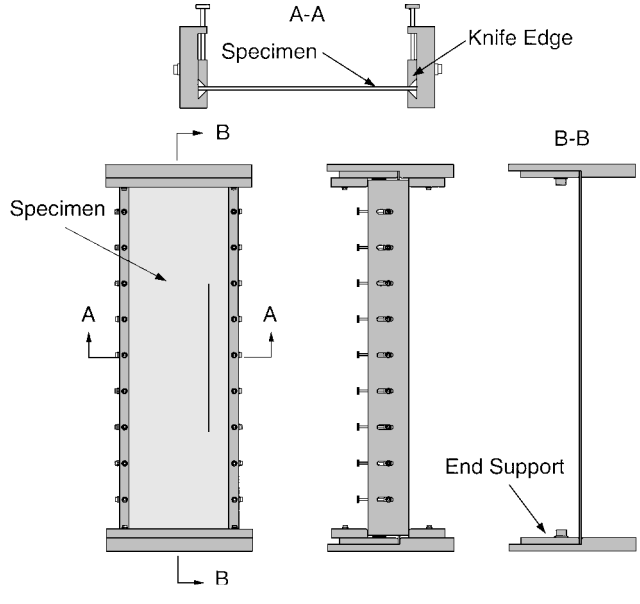

Fig. 4 Schematic of the load introduction fixture.

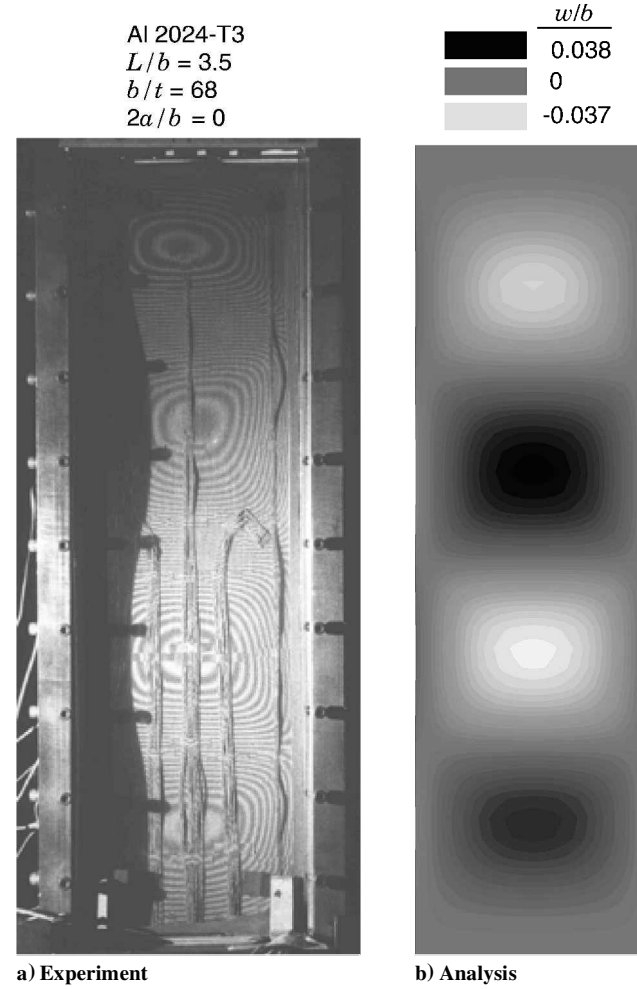

Fig. 5 Qualitative comparison of out-of-plane deflections for a plate with no crack.

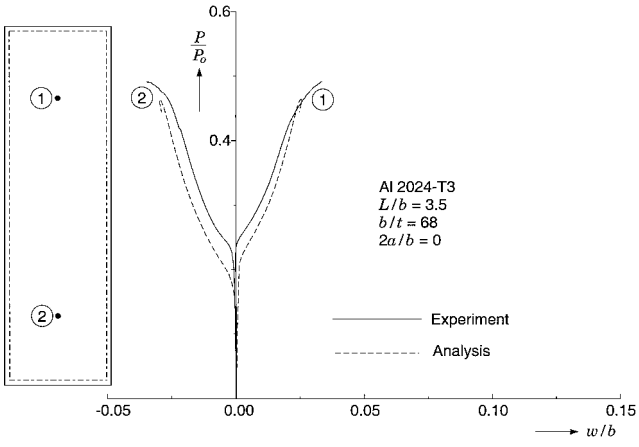

Fig. 6 Quantitative comparison between experiment and analysis of out-of-plane deflections at two points for a plate with no crack.

measurements. Both responses have a pattern with one half-wave across the width and four half-waves along the length. A quantitative comparison of the out-of-plane deflection measured at the two points indicated in the insert and the calculated results is presented in Fig. 6. The calculations compare favorably to the experimental measurements. The calculated bifurcation load for the plates is $P_b/P_o = 0.202$, which is the approximate load for which the lateral deflections start developing significantly in both the experimental and numerical results. The numerical results predict loads that are somewhat lower in value than the experimental results and yield a value for the limit load of $P_L/P_o = 0.492$. This plate was loaded in load control during the experiment, and so the limit load was not identified (although the curves suggest the limit load is not much higher than the maximum load recorded). The capability of the simulations to calculate the limit load will be assessed in the next two cases.

The second specimen tested contained a longitudinal crack with length $2a/b = 1.73$ centered in the plate. Loading for this experiment was accomplished by axial displacement control. A qualitative comparison of the measured and calculated out-of-plane deflections of this plate is shown in Fig. 7. (The experimental fringe pattern corresponds to a load of $P/P_o = 0.384$ because the fringes at the limit load were too closely spaced to be reproduced clearly. The contour plot obtained from the analysis corresponds to the limit load.) The mode of deformation is different from that of the plate without a crack, and the numerical results represent the difference. As in the preceding case, the out-of-plane displacements are nearly symmetric about the center of the plate. The displacement patterns above and below the crack differ somewhat between the experimental results and the numerical prediction. Most likely this difference is caused by unavoidable differences in boundary conditions between experiment and analysis. Quantitative comparisons between the measured and calculated load vs out-of-plane displacement curves are shown in Fig. 8 for the points indicated in the insert. The bifurcation buckling load occurs at $P_b/P_o = 0.110$. The out-of-plane displacements develop more gradually for the experimental results, but the overall agreement between experimental and numerical results is good. The numerically calculated limit load is $P_L/P_o = 0.466$. The measured and calculated limit loads are within 2% of each other in this case. The calculated limit load is just 5% less than the value computed for the plate without a crack, although the bifurcation load is only 54% of that for the uncracked plate.

The third specimen contained a crack with the same length as the preceding case, but the crack was located toward the edge of the plate so that $2e/b = 0.67$. A comparison of the experimental and analytical out-of-plane displacements at the limit load is shown in Fig. 9. The out-of-plane displacements of the interior of the plate are much larger than the part of the plate near the boundary. Again, qualitatively, the measured and calculated out-of-plane displacement patterns are in good agreement.

Quantitative comparisons of the measured and calculated out-of-plane displacements are shown in Fig. 10 at the three points

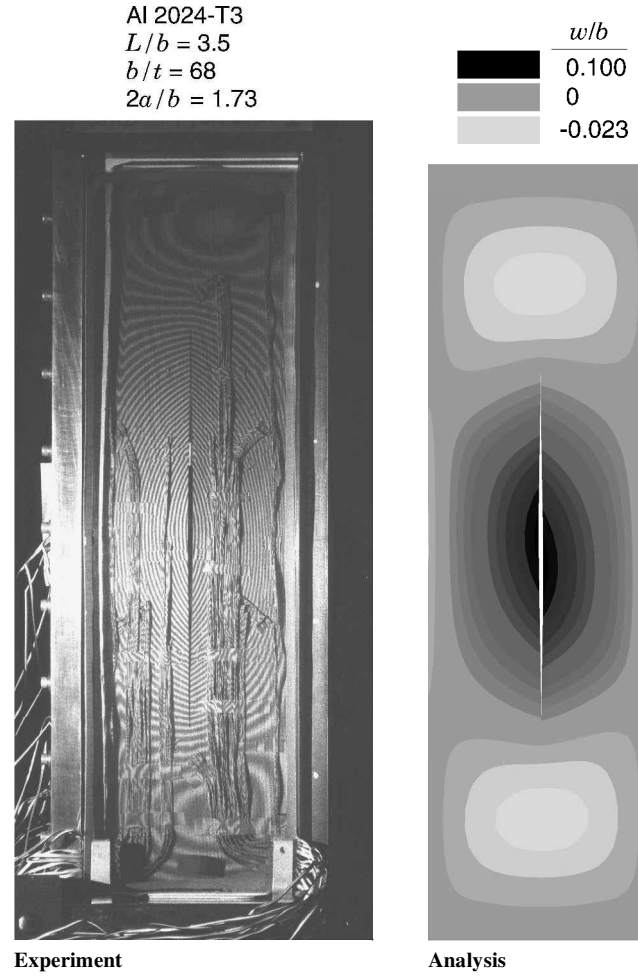

Fig. 7 Qualitative comparison of out-of-plane deflections for a plate with a centered crack.

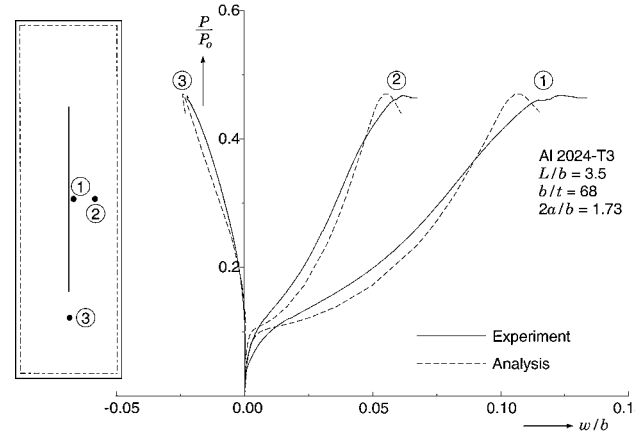

Fig. 8 Quantitative comparison between experimental and analytical out-of-plane deflections at three points for a plate with a centered crack.

indicated in the insert. These results compare reasonably well. The calculated bifurcation buckling load is $P_b/P_o = 0.064$. Indeed, the measured and calculated out-of-plane displacements at point 1 start developing at that load level. The comparison between calculated and measured responses remains good. The analysis predicts the limit load to be $P_L/P_o = 0.403$, which is approximately 9% larger than the measured value.

The experimental and numerical results indicate that moving the crack closer to the edge of the plate causes a reduction in the collapse load. Several factors contribute to this effect. First, the bifurcation buckling load is significantly lower for plates with cracks near the

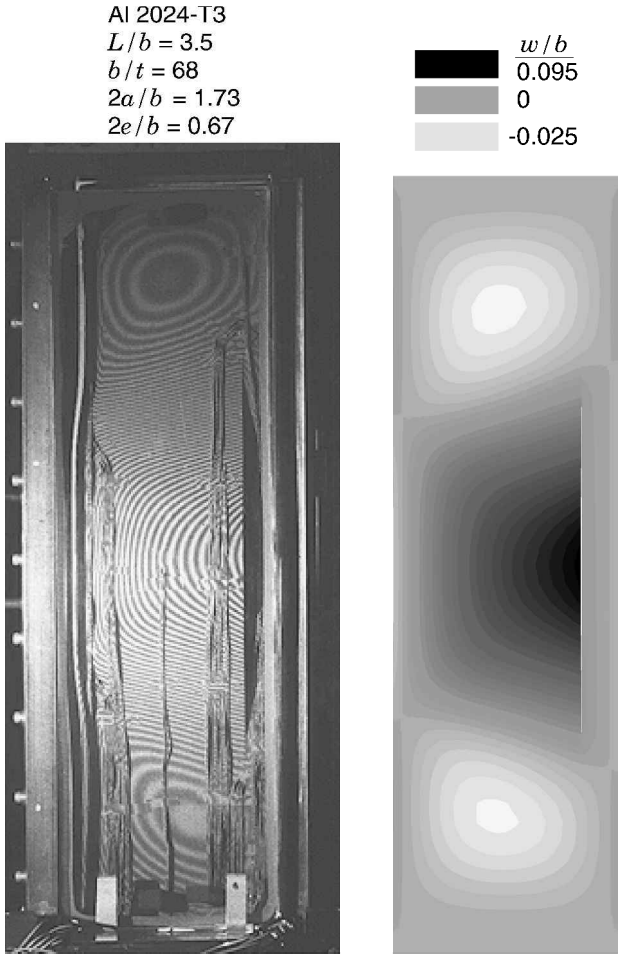

Fig. 9 Qualitative comparison of out-of-plane deflections for a plate with a side crack.

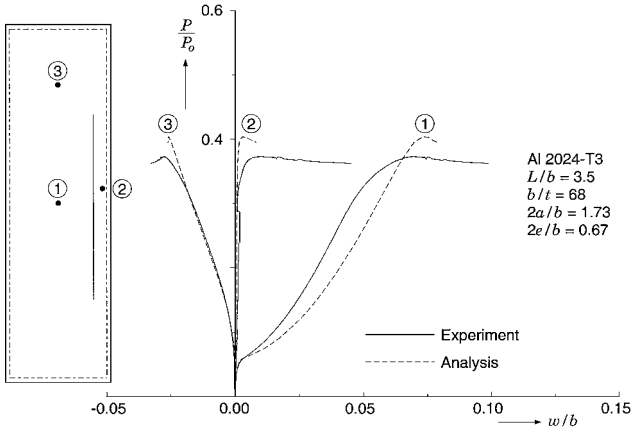

Fig. 10 Quantitative comparison between experimental and analytical out-of-plane deflections at three points for a plate with a side crack.

edge. As a result, out-of-plane displacements begin increasing at a lower load, and the postbuckling response is axially less stiff. (For example, compare the postbuckling responses in Figs. 3b and 3c.) These effects cause yielding to occur at a lower value of load. In addition, the difference in the transverse displacements of the plate to the left and right of the crack become more pronounced, which increases the stress at the crack tip and precipitates yielding. Finally, the crack is closer to the edge of the plate, where edge effects also tend to increase the stress levels. These combined effects contribute to more severe plastic deformation, which reduces the value of the collapse load.

The equivalent stress contour plots at collapse reveal that the maximum equivalent stresses in all three cases are on the order of 380 MPa (55 ksi). From Fig. 2 the largest equivalent strains at collapse are on the order of 2%.

Parametric Study

The comparison of the experimental and numerical results shows good agreement. Therefore, a numerical parametric study of the problem using STAGS should yield results that are indicative of the response of rectangular plates containing longitudinal cracks with similar orientation as those considered in the experiments.

The model for the parametric study is that shown in Fig. 1. Even for such a relatively simple problem, the number of parameters that can be varied is large. These include geometric parameters L/b and b/t; crack parameters such as $2a/b$, $2e/b$, and the axial location of the center of the crack; in-plane and out-of-plane boundary conditions at each of the four edges; initial geometric imperfection shape and amplitude; and the shape of the stress-strain curve. The parameters fixed and varied in this study are described next.

The ratio b/t was fixed at a value of 66.7. Variation of this parameter can alter the behavior of the plates in two ways. For larger b/t values mode jumping instabilities can become an issue. These instabilities can be determined with STAGS as shown in Ref. 13 and demonstrated for the current problem by the results in Ref. 14. The computational effort, however, becomes very large because the dynamic, transient response of the plates during the mode jumps must be calculated. The results in Ref. 14 indicate that the dependence of the collapse load on crack length and position for plates with larger b/t is likely to be similar to that presented in this study. For lower values of b/t, it is possible for the bifurcation buckling load to occur in the plastic range. For the material considered in this study, a short calculation indicates that, for a fully clamped plate without a crack, the value of b/t should remain greater than 36 for buckling to occur in the elastic range if $L/b = 4$, which is the aspect ratio considered for most of this study.

The stress-strain curve used is shown in Fig. 2. The slope of the elastic region (Young's modulus) influences the value of the bifurcation buckling load of the plate, whereas the collapse loads are further influenced by the yield stress and the postyield hardening characteristics. Yielding will also be considered to be isotropic in all cases. Finally, exploratory calculations indicate that the axial position of the crack does not significantly influence the results. The parameters varied in the study include the aspect ratio L/b, the crack length $2a/b$, the lateral crack position $2e/b$, the in-plane and out-of-plane boundary conditions, and the amplitude of the initial geometric imperfections of the plates. The out-of-plane boundary conditions are always the same on all four sides for this study. The in-plane boundary conditions are only varied along the sides of length L.

The parametric study was conducted with STAGS using the same two-step process and plate dimensions already presented in the discussion of Fig. 3.

Effect of Crack Length and In-Plane Boundary Conditions

Typical axial load-deflection responses of clamped plates with crack length $2a/b = 1$ are shown in Fig. 3b for plates with centered cracks ($2e/b = 0$) and in Fig. 3c for plates with cracks at the edge ($2e/b = 1$). In those examples the long edges of the plate remain straight and vertical at all times. The results indicate that the collapse load of the plate is not affected significantly by the crack if the crack is located at the center of the plate, but it decreases considerably if the crack is located at the edge of the plate. A summary of the effect of crack length on the bifurcation and collapse loads for these two crack locations is shown in Fig. 11. It has been shown[15] that although the in-plane boundary conditions do not affect the bifurcation load they can affect the elastic postbuckling response. As a result, these boundary conditions can also affect the yield and collapse loads of the plates. Therefore, Fig. 11 shows results for two types of in-plane boundary conditions: one with the edges of length L straight (to simulate a plate bounded by heavy stiffeners) and one with the same edges free to deflect (as in the experiments). In both cases the

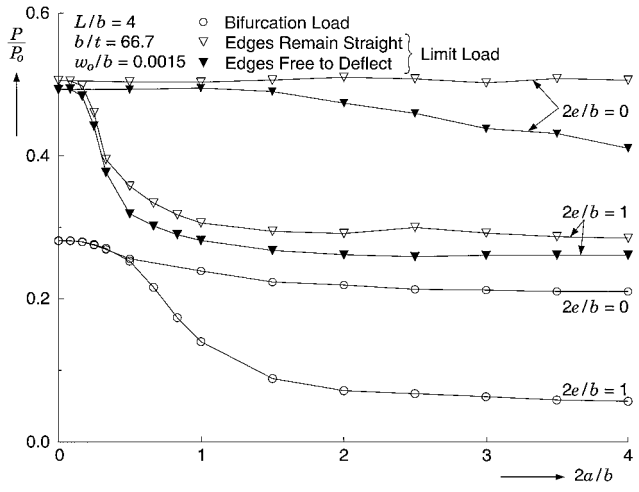

Fig. 11 Bifurcation and collapse loads for clamped plates with cracks at the center ($2e/b = 0$) or edge ($2e/b = 1$) as a function of crack length.

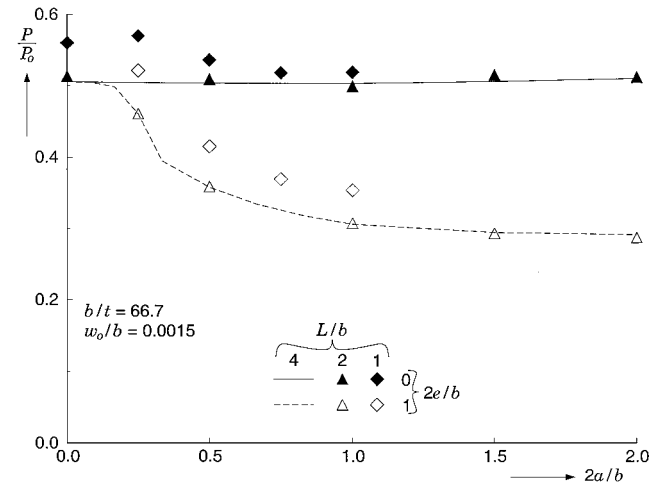

Fig. 12 Bifurcation and collapse loads for clamped plates with straight edges and cracks at the center ($2e/b = 0$) or edge ($2e/b = 1$) as function of crack length for three values of L/b.

resultant lateral load in the plates is equal to zero, but in the first case the lateral stress resultant N_x might be nonzero at these edges, whereas for the latter case N_x is equal to zero.

The bifurcation load decreases as the crack length $2a/b$ increases for both crack locations as shown in Fig. 11. (The calculated points have been joined by straight lines in the figure as a means of grouping the results. The actual plots of results between points can exhibit discontinuities in slope. Therefore, the lines in the figure do not imply interpolation of the results.) The decrease in bifurcation load is much more severe when the crack is located near the edge of the plate. Most of the decrease in load occurs in the range $2a/b < 1.5$, and the bifurcation load becomes virtually independent of crack length for longer cracks.

The collapse loads are somewhat dependent on the in-plane boundary conditions. The results for plates with $2e/b = 0$ and edges that remain straight (open symbols) indicate that the collapse load is relatively insensitive to crack length. The corresponding results for edges free to deform (filled symbols) display somewhat lower collapse loads and a slow decrease in collapse load for longer crack lengths. If the crack is located at the edge of the plate, however, the results for both types of boundary conditions show a sharp decrease in collapse load for progressively longer cracks in the range $2a/b < 1$, followed by a relative insensitivity to longer cracks. The reduction in collapse load is more precipitous than the reduction in the first bifurcation load, and the plate with edges free to deform has somewhat lower collapse loads. The presence of cracks with $2e/b = 1$ and $2a/b > 1$ reduces the collapse load of the plates to the level of the bifurcation load of the plate with no crack.

Effect of Aspect Ratio

The effect of aspect ratio L/b on the collapse load as a function of crack length for plates with edges that remain straight is shown in Fig. 12. The results for $L/b = 4$ from Fig. 11 are shown as continuous lines, results for plates with $L/b = 2$ are shown by triangles, and those for $L/b = 1$ by diamonds. The results for plates with $L/b = 2$ and 4 are virtually the same. Plates with $L/b = 1$ exhibit somewhat higher collapse loads. These results imply that the results of the rest of the parametric study, conducted for plates with $L/b = 4$, are valid for long plates with $L/b \geq 2$ if the crack length is normalized by the width of the plate b. The results also indicate that, for cracks with $2e/b = 1$, the decrease in collapse load with increasing crack length occurs in the range $2a/b < 1$.

Effect of Crack Lateral Position

The axial load-deflection response of plates that have equal crack lengths of $2a/b = 1$ but with the cracks at different lateral positions $2e/b$ is shown in Fig. 13. All four edges of the plates are restrained against out-of-plane displacements. The in-plane boundary conditions require the edges to remain straight. The plots for all cases are virtually identical and linear at low values of loads. Once the

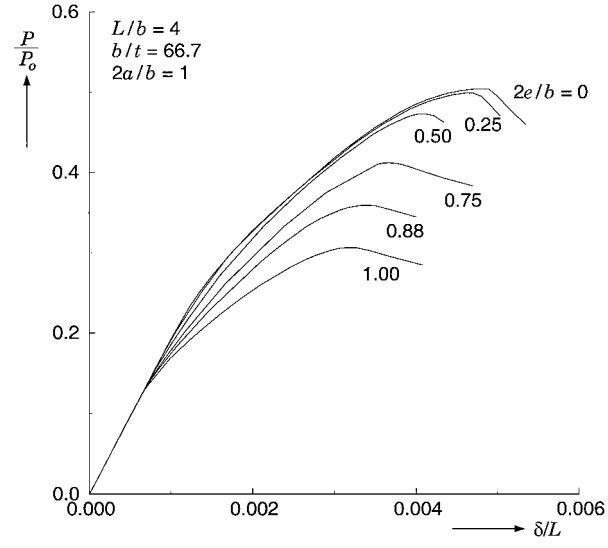

Fig. 13 Effect of crack lateral position on the axial load-deflection response of clamped plates with straight edges.

load in each case reaches the bifurcation load, the responses become nonlinear, and each follows a different path. The bifurcation load decreases as $2e/b$ increases. Similarly, the limit loads decrease as the crack locations move to the side of the plate. The decrease in collapse load is relatively minor for the cases where $2e/b < 0.5$. The decrease accelerates as the crack is located closer to the edge of the plate.

Effect of Initial Geometric Imperfections

It has been shown that the collapse of the plates considered in the present study is a result of the interaction of geometric nonlinearities with the elastic-plastic response of the material. The development of the geometric nonlinearities is influenced by the initial geometric imperfections of the plates, and as a result some influence can be expected on the collapse load. The results of a parametric study of the effect of initial imperfection amplitude on the axial load-deflection response of the plates are presented in Fig. 14. The shape of the imperfections used to generate the results shown in Figs. 14a and 14b remain as explained earlier. This imperfection produces somewhat random results for the cases shown in Fig. 14c. The results have a more definite trend if the shape of the imperfection is restricted to that of the first buckling mode only. The first mode shape was used as an imperfection in this case. The plates are clamped for all cases presented, and the in-plane boundary conditions require that the edges of the plates remain straight.

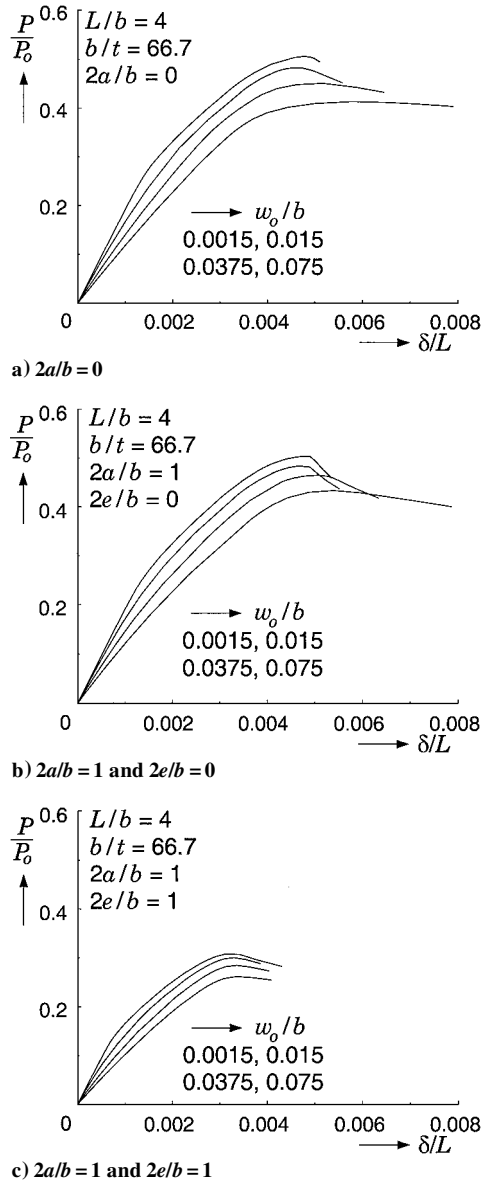

Fig. 14 Effect of initial geometric imperfection amplitude on the axial load-deflection response of clamped plates with straight edges.

The results for a plate without a crack are shown in Fig. 14a. The smallest imperfection amplitude has been used for all results presented earlier. An increasing imperfection amplitude results in a decrease in the load for the initial responses, whose slopes tend toward the postbuckling slope of the case with the smallest imperfection amplitude. The collapse load also decreases with increasing imperfection amplitude. The decrease, however, is relatively moderate considering that the range of imperfection amplitudes covered 1.5 orders of magnitude. Results for plates with cracks with length $2a/b = 1$ and $2e/b = 0$ and 1, respectively, are presented in Figs. 14b and 14c. As in the case with a plate with no crack, the imperfection sensitivity is moderate for the parameters considered.

Effect of Out-of-Plane Boundary Conditions

A comparison of the bifurcation and collapse loads of plates with clamped and simply supported out-of-plane boundary conditions is shown in Fig. 15 as a function of crack length. The in-plane boundary conditions require that the edges of the plates remain straight in both cases. The bifurcation and collapse load trends are, for the most part, similar for both boundary conditions. The magnitudes of the bifurcation and collapse loads, however, are in general smaller if the edges are simply supported rather than clamped. The results for simply supported boundary conditions show some irregularity in the collapse loads for plates with very short cracks because of mode

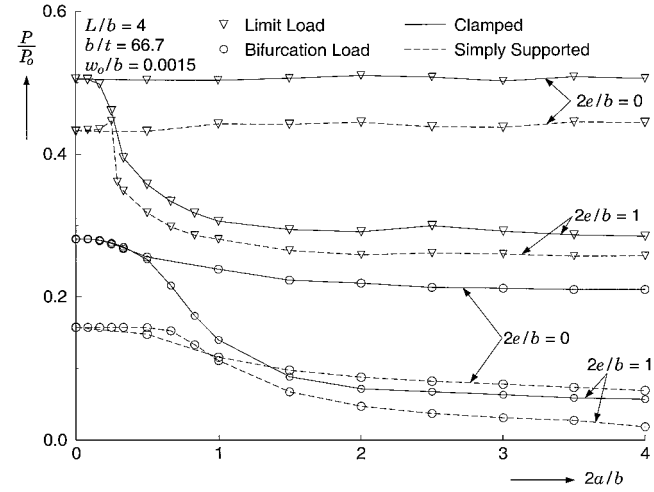

Fig. 15 Comparison of bifurcation and collapse loads for clamped and simply supported plates with straight edges as a function of crack length.

jump instabilities that occur for these plates. The results for the two cases with shortest cracks involved calculating the dynamic, transient response during the mode jumps. Note that the residual strength of simply supported plates with $2e/b = 1$ and $2a/b > 1$ is substantially greater than the bifurcation buckling load of the plate without a crack, unlike the clamped plates.

Conclusions

A limited experimental study combined with numerical simulations was conducted to determine the response and stability characteristics of elastic-plastic rectangular aluminum plates with longitudinal cracks and subjected to uniaxial compression loads. A parametric study of the problem was also performed to determine the sensitivity of the results to changes in the plate parameters. The response of such plates is characterized by bifurcation and limit load instabilities. The limit load induces collapse and is the result of the interaction between geometric nonlinearities and the elastic-plastic response of the material.

For the cases considered in the experiments, introduction of a crack with $2a/b = 1.73$ and $2e/b = 0$ resulted in little decrease in the collapse load in comparison to the plate without a crack. Here $2a$ is the crack length, b is the width of the plate, and e is the distance between the crack and the longitudinal centerline of the plate. This result is likely caused by the well-known fact that plates in the postbuckling regime redistribute their internal load to regions near the longitudinal edges. Hence the presence of a crack at the center of the plate does not seriously degrade the collapse load. The collapse load decreases, however, when the crack location is near an edge (for example, $2e/b = 1$). The reasons for the decrease in collapse load include a lower bifurcation load, a more flexible postbuckling response, and a more severe state of stress near the crack tips that promotes plastic deformation. The numerical simulation of the experiments yielded results that are quantitatively in good agreement with the experimental results. The numerical results reflected the decrease in collapse load when the crack is near the edge.

The parametric study provided further information regarding the dependence of the bifurcation and collapse loads of the plates on crack length and position, aspect ratio, boundary conditions, and initial geometric imperfection amplitude. The results of the parametric study support the observation made during the experiments that cracks located at the center of the plate have little effect on the collapse load regardless of whether the plates were simply supported or clamped on all four edges. This observation is particularly true if the in-plane boundary conditions require the edges of the plates to remain straight. A moderate decrease in collapse load was identified if the edges of the plate were free to deform. The collapse load of the plates, however, becomes sensitive to crack length if the crack is located at the edges of the plate. In this case the presence of the crack can reduce the collapse load by as much as 40% of that of a plate without a crack. The reduction in collapse load takes place in

the crack length range $2a/b < 1$; longer cracks do not significantly reduce the collapse load further. The collapse load was found to be moderately imperfection sensitive. The presence and location of the crack did not appear to change the imperfection sensitivity of the collapse load significantly for the cases considered.

Acknowledgments

The support of the NASA Langley Research Center for the work conducted at Notre Dame through Grants NAG1-2032 and NAG1-2214 is acknowledged with thanks. Special thanks to Richard D. Young for his help in the course of this study. The assistance of Heidi Orde in generating STAGS results is also acknowledged with thanks.

References

[1]Goranson, U. G., "Fatigue Issues in Aircraft Maintenance and Repairs," *International Journal of Fatigue*, Vol. 20, No. 6, 1997, pp. 413–431.

[2]Starnes, J. H., Britt, V. O., and Rankin, C. C., "Nonlinear Response of Damaged Stiffened Shells Subjected to Combined Internal Pressure and Mechanical Loads," *Proceedings of the AIAA/ASME/ASCE/AHS/ASC 36th Structures, Structural Dynamics, and Materials Conference*, AIAA, Washington, DC, 1995, pp. 2700–2712.

[3]Starnes, J. H., Britt, V. O., Rose, C. A., and Rankin, C. C., "Nonlinear Response and Residual Strength of Damaged Stiffened Shells Subjected to Combined Loads," *Proceedings of the AIAA/ASME/ASCE/AHS/ASC 37th Structures, Structural Dynamics, and Materials Conference*, AIAA, Reston, VA, 1996, pp. 2096–2111.

[4]Starnes, J. H., and Rose, C. A., "Nonlinear Response of Thin Cylindrical Shells with Longitudinal Cracks and Subjected to Internal Pressure and Axial Compression Loads," *Proceedings of the AIAA/ASME/ASCE/AHS/ASC 38th Structures, Structural Dynamics, and Materials Conference*, AIAA, Reston, VA, 1997, pp. 2213–2223.

[5]Borgan, F. A., Rankin, C. C., Cabiness, H. D., and Loden, W. A., "STAGS User Manual, Version 2.3," Lockheed Martin Missiles and Space Co., Inc., Palo Alto, CA, July 1996.

[6]Rankin, C. C., and Brogan, F. A., "The Computational Structural Mechanics Testbed Structural Processor ES5: STAGS Shell Element," NASA CR 4358, May 1991.

[7]Besseling, J. F., "A Theory of Elastic, Plastic and Creep Deformations on an Initially Isotropic Material Showing Anisotropic Work-Hardening, Creep Recovery and Secondary Creep," *Journal of Applied Mechanics*, Vol. 25, No. 4, 1958, pp. 529–536.

[8]Zienkiewicz, O. C., Nayak, G. C., and Owen, D. R. J., "Composite and 'Overlay' Models in Numerical Analysis of Elasto-Plastic Continua," *Foundations of Plasticity*, edited by A. Sawczuk, Noordfhoff International, Leyden, The Netherlands, 1972, pp. 107–122.

[9]Brush, D. O., and Almroth, B. B., *Buckling of Bars, Plates and Shells*, McGraw–Hill, New York, 1975, pp. 113–116.

[10]Stein, M., "Loads and Deformations of Buckled Rectangular Plates," NASA TR R-40, 1959.

[11]Goodemote, D. P., "Response and Failure of Rectangular Plates Under Biaxial Load," M.S. Thesis, Structural/Solid Mechanics Lab., Rept. 00/4, Univ. of Notre Dame, Notre Dame, IN, Dec. 2000.

[12]"NASA/Aircraft Industry Standard Specification for Graphite Fiber/Toughened Thermoset Resin Composite Material," NASA RP 1142, June 1985.

[13]Riks, E., "Buckling Analysis of Elastic Structures: A Computational Approach," *Advances in Applied Mechanics*, Vol. 34, edited by E. van der Giessen, and T. Y. Wu, Academic Press, San Diego, CA, 1998, pp. 1–76.

[14]Corona, E., "Collapse of Elastic-Plastic Plates with Cracks," *Proceedings of the 41st AIAA/ASME/ASCE/AHS/ASC Structures, Structural Dynamics, and Materials Conference*, Vol. 1, Pt. 2, AIAA, Reston, VA, 2000, pp. 1416–1420.

[15]Supple, W. J., and Chilver, A. H., "Elastic Postbuckling of Compressed Rectangular Flat Plates," *Thin Walled Structures*, edited by A. H. Chilver, Wiley, New York, 1967, pp. 136–152.

A. N. Palazotto
Associate Editor